

## ION HEATING BY A SPECTRUM OF OBLIQUELY PROPAGATING LOW-FREQUENCY ALFVÉN WAVES

QUANMING LU<sup>1</sup> AND LIU CHEN<sup>2,3</sup>

<sup>1</sup> CAS Laboratory of Basic Plasma Physics, School of Earth and Space Sciences, University of Science and Technology of China, Hefei 230026, China

<sup>2</sup> Institute for Fusion and Simulation, Zhejiang University, Hangzhou 310027, China

<sup>3</sup> Department of Physics and Astronomy, University of California, Irvine, CA 92697, USA

Received 2009 May 5; accepted 2009 August 31; published 2009 September 24

### ABSTRACT

Ion stochastic heating by a monochromatic Alfvén wave, which propagates obliquely to the background magnetic field, has been studied by Chen et al. It is shown that ions can be resonantly heated at frequencies a fraction of the ion cyclotron frequency when the wave amplitude is sufficiently large. In this paper, the monochromatic wave is extended to a spectrum of left-hand polarized Alfvén waves. When the amplitude of the waves is small, the components of the ion velocity have several distinct frequencies, and their motions are quasi-periodic. However, when the amplitude of the waves is sufficiently large, the components of the ion velocity have a spectrum of continuous frequencies near the ion cyclotron frequency due to the nonlinear coupling between the Alfvén waves and the ion gyromotion, and the ion motions are stochastic. Compared with the case of a monochromatic Alfvén wave, the threshold of the ion stochastic heating by a spectrum of Alfvén waves is much lower. Even when their frequencies are only several percent of the ion cyclotron frequency, the ions can also be stochastically heated. The relevance of this heating mechanism to solar corona is also discussed.

*Key words:* solar wind – Sun; corona – waves

### 1. INTRODUCTION

Alfvén waves are considered to play a crucial role in heating of plasmas, such as the solar corona and magnetic fusion devices (Nekrasov 1970; Hollweg 1978; Lieberman & Lichtenberg 1973; Karney 1979; Abe et al. 1984). Numerous theoretical and experimental papers have been published to investigate resonant heating of ions by Alfvén waves (Isenberg & Hollweg 1983; Cranmer et al 1999; Li et al. 1999; Tu & Marsch 2001; Lu et al. 2006a, 2006b). In these works, the cyclotron resonant condition ( $\omega - k_{\parallel}v_{\parallel} = n\Omega_0$ , where  $n$  is an integer,  $\omega$  and  $\mathbf{k}$  are the frequencies and wavevectors of the Alfvén waves, respectively.  $\mathbf{v}$  is the particle velocity in the laboratory frame. The subscript “ $\parallel$ ” denotes the component parallel to the background magnetic field and  $\Omega_0$  is the cyclotron frequency of the particle) is necessary for ion heating by the Alfvén waves, and in general the frequencies of the applied Alfvén waves are comparable to the cyclotron frequency. Recently, Chen et al. (2001) found that an obliquely propagating Alfvén wave with sufficiently large amplitude can break the magnetic moment invariant at frequencies a fraction of the ion cyclotron frequency, and thus ion stochastic heating by such sub-cyclotron resonance at low frequencies is possible. Guo et al. (2008) further pointed out that the ion heating occurs when the cyclotron resonances at sub-cyclotron frequencies start to overlap with their corresponding neighboring resonances and then leads to global stochasticity. When a spectrum of Alfvén waves is considered, White et al. (2002) demonstrated that the amplitude threshold of the Alfvén waves for ion stochastic heating can be significantly decreased. Evidences of ion heating by low-frequency Alfvén waves have also been found in laboratory experiments (Gates et al. 2001; Fredrickson et al. 2002; Zhang et al. 2008).

In the present paper, with test particle calculations we investigate ion stochastic heating by a spectrum of obliquely propagating Alfvén waves with left-hand polarization. By analyzing the spectrum of the components of the ion velocity as well as the evolution of the ion temperature, a more precise determina-

tion of the threshold for ion stochastic heating for a spectrum of oblique Alfvén waves is investigated.

The paper is organized as follows. In Section 2, the simulation model is presented, and the simulation results are described in Section 3. In Section 4, we discuss and summarize our results.

### 2. SIMULATION MODEL

A spectrum of left-hand circularly polarized Alfvén waves is considered in this paper, and the waves propagate obliquely to the background magnetic field. The dispersion relation of the Alfvén waves is  $\omega = k_z v_A$ , where  $v_A = B_0 / (4\pi n_0 m_i)^{1/2}$  is the Alfvén speed and the background magnetic field is  $\mathbf{B}_0 = B_0 \mathbf{i}_z$ . Thus, in the wave frame we have the wave magnetic field (Chen et al. 2001)

$$\mathbf{B}_w = \sum_{k=1}^N B_k [-\cos(\alpha) \sin(\psi_k) \mathbf{i}_x + \cos(\psi_k) \mathbf{i}_y + \sin(\alpha) \sin(\psi_k) \mathbf{i}_z], \quad (1)$$

where  $\psi_k = k_x x + k_z z + \varphi_k$ ,  $\tan(\alpha) = k_x / k_z$ , and  $\varphi_k$  is the random phase for mode  $k$ .  $N$  is the number of wave modes. The particles move in the magnetic field as described by the following equations:

$$m_i \frac{d\mathbf{v}}{dt} = q_i \mathbf{v} \times (\mathbf{B}_0 + \mathbf{B}_w), \quad (2)$$

$$\frac{d\mathbf{r}}{dt} = \mathbf{v}, \quad (3)$$

where the subscript  $i$  indicates physical quantities associated with ion species  $i$ . In this paper, we consider particle motions in the wave frame and the wave electric field is eliminated. The equations are solved with Boris algorithm (Birdsall & Langdon, 2005), where the kinetic energy of the particle is conserved in the calculation of cyclotron motion. The time step is  $\Omega_p t = 0.025$ , where  $\Omega_p$  is the proton cyclotron frequency.

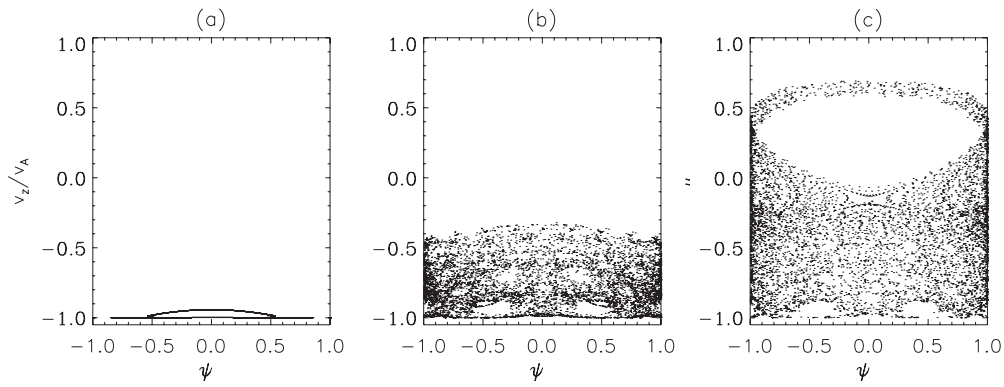


**Figure 1.** Poincaré plot for a monochromatic Alfvén wave, and the parameters are  $\omega = 0.25$ ,  $\alpha = 45^\circ$ , and (a)  $B_k^2/B_0^2 = 0.02$ , (b)  $B_k^2/B_0^2 = 0.067$ , and (c)  $B_k^2/B_0^2 = 0.08$ .

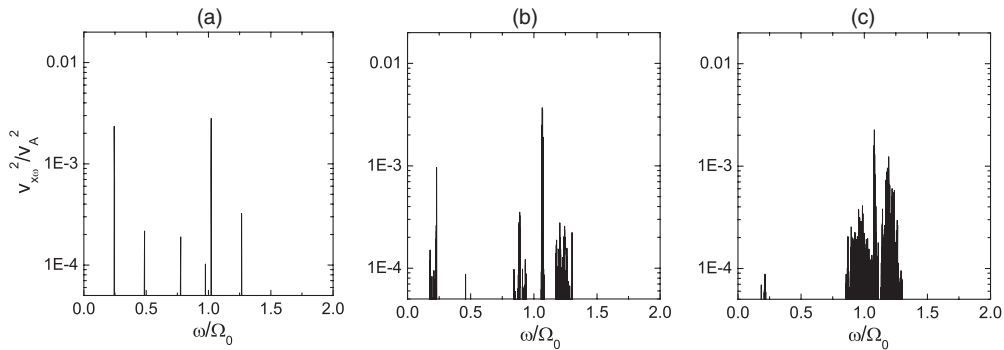


**Figure 2.** Power spectrum of the  $x$  component of the ion velocity  $v_x(t)$ , which is obtained by FFT the time series of  $v_x(t)$  from  $\Omega_p t = 0$  to  $\Omega_p t = 26214.4$ . The parameters are the same as in Figure 1.

### 3. SIMULATION RESULTS

In the laboratory frame the waves propagate in the positive  $z$  direction, whose phase velocity is equal to the Alfvén speed  $v_A$ . Therefore, in the wave frame an initially cold ion distribution has velocity  $v_x = 0$ ,  $v_y = 0$ , and  $v_z = -v_A$ . In this paper, we investigate the effects of the number of wave modes on ion heating by the oblique Alfvén waves. At first, we show the results for the monochromatic wave, and then the effects of the number of wave modes on ion heating are investigated

#### 3.1. The Monochromatic Alfvén Wave

To study ion heating, a Poincaré plot of  $\lambda = v_z/v_A$ ,  $\psi_B = \cos(k_x x + k_z z + \varphi_k)$ , formed by taking points when  $v_y = 0$  and  $\dot{v}_y > 0$ , is constructed in the wave frame. Poincaré plot is the intersection of an orbit in the state space of a continuous dynamical system with a certain lower dimensional subspace, called the Poincaré section. Poincaré plot preserves many properties of orbits of the original dynamical system and has a lower dimensional state space. Therefore, it is a useful tool to analyze the properties of a dynamical system (Lieberman & Lichtenberg, 1983). Figure 1 describes the Poincaré plot for a monochromatic Alfvén wave, and the parameters are  $\omega = 0.25\Omega_p$ ,  $\alpha = 45^\circ$ , and (a)  $B_k^2/B_0^2 = 0.02$ , (b)  $B_k^2/B_0^2 = 0.067$ , and (c)  $B_k^2/B_0^2 = 0.08$ . With the increase of the wave amplitude, the motions of the ion become stochastic due to the resonance with the wave at sub-cyclotron frequencies, and the threshold is about  $B_k^2/B_0^2 = 0.067$  (correspondingly,  $B_k/B_0 \approx 0.259$ , which is consistent with the results of Chen et al. 2001). When the amplitude is  $B_k^2/B_0^2 = 0.08$ , the ion can readily diffuse from  $v_z = -v_A$  to about  $v_z = 0.7v_A$ , and its motions are stochastic.

The ion stochastic motions can also be demonstrated in Figure 2, which shows the power spectrum of the  $x$  component of the ion velocity  $v_x(t)$ . We first obtain a time series of  $v_x(t)$  from  $\Omega_p t = 0$  to  $\Omega_p t = 26214.4$  by solving Equations (2) and (3), and then calculate its power spectrum by Fast Fourier Transform (FFT) the time series of  $v_x(t)$ . The parameters are the same as in Figure 1. When the wave amplitude is small ( $B_k^2/B_0^2 = 0.02$ ), the ion motions have two main frequencies: one is near  $0.25\Omega_p$  and the other is near  $1.0\Omega_p$ . These two frequencies correspond to the frequencies of the Alfvén wave and ion gyromotion, respectively, and the ion motions are quasi-periodic. With the increase of the wave amplitude, the ion motions have more and more distinct frequencies. When the wave amplitude is sufficiently large, the ion motions have a continuous frequency spectrum, which is stochastic. For the case  $B_k^2/B_0^2 = 0.08$ , the main frequencies are concentrated between  $0.8\Omega_p$  and  $1.3\Omega_p$  with a continuous spectrum. Consistent with the results of Poincaré plot and the plot of  $x-v_x$ , the threshold of the ion stochastic motions is around  $B_k^2/B_0^2 = 0.067$ .

Figure 3 shows the time evolution of the parallel and perpendicular temperatures for the wave amplitude  $B_k^2/B_0^2 = 0.02$  and  $B_k^2/B_0^2 = 0.08$ . In the figure, A and B denote  $T_{\parallel}/T_{\parallel 0}$  and  $T_{\perp}/T_{\perp 0}$  for amplitude  $B_k^2/B_0^2 = 0.02$ , while C and D denote  $T_{\parallel}/T_{\parallel 0}$  and  $T_{\perp}/T_{\perp 0}$  for amplitude  $B_k^2/B_0^2 = 0.08$ . Here, the subscript “0” stands for the initial values of physical quantities. Initially, particles are evenly distributed in a region with size  $24\pi \times 24\pi$  in the  $z-x$  plane, and the region is divided into  $48 \times 48$  grids. The thermal velocity of the particles is  $0.1v_A$ , and there is no drift velocity in the laboratory frame. The total number of particles is 230,400. Double periodic boundary conditions are used for the particles: if one

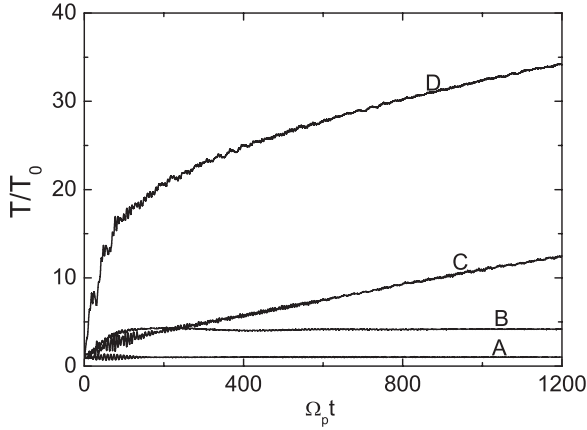


**Figure 3.** Time evolution of the parallel and perpendicular temperatures for the wave amplitude  $B_k^2/B_0^2 = 0.02$  and  $B_k^2/B_0^2 = 0.08$ . A monochromatic Alfvén wave with  $\omega = 0.25$ ,  $\alpha = 45^\circ$  is used. In the figure, A and B denote  $T_{\parallel}/T_{\parallel 0}$  and  $T_{\perp}/T_{\perp 0}$  for amplitude  $B_k^2/B_0^2 = 0.02$ , while C and D denote  $T_{\parallel}/T_{\parallel 0}$  and  $T_{\perp}/T_{\perp 0}$  for amplitude  $B_k^2/B_0^2 = 0.08$ .

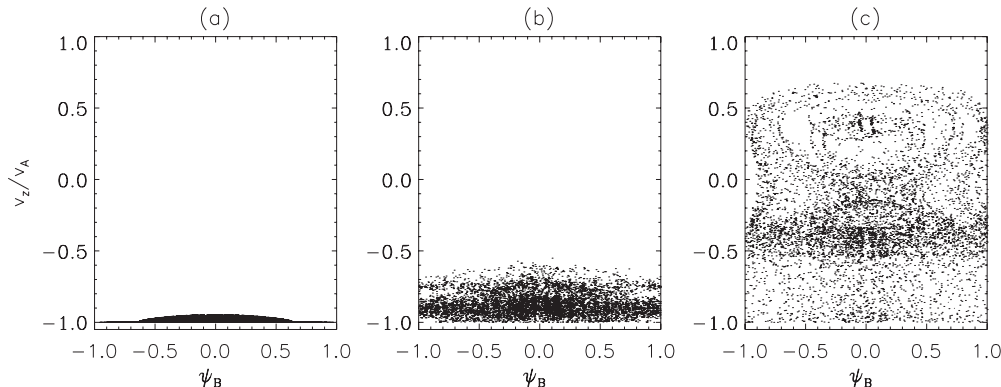
moves out of one boundary, it will enter from the opposite boundary. In this and the following subsections, we calculate the parallel and perpendicular temperatures using the following procedure: we first calculate  $T_{\parallel} = m_i/k_B \langle (v_z - \langle v_z \rangle)^2 \rangle$ ,  $T_{\perp} = m_i/2k_B \langle (v_x - \langle v_x \rangle)^2 + (v_y - \langle v_y \rangle)^2 \rangle$  in every grid (where the bracket  $\langle \bullet \rangle$  denotes an average over a grid cell), and then the temperatures are averaged over all grids. In this way, we can eliminate the effects of the average velocity at each location on the thermal temperature. From the figure, we can find that ions can be rapidly heated before  $\Omega_p t \approx 100$ , and such mechanism to heat the ions is due to the phase mixing between ions, which has been discussed in Lu & Li (2007) and Li et al. (2007). In the process of phase mixing, ions are first picked up in the transverse direction by the Alfvén wave and obtain an average transverse velocity, then the parallel thermal motions of ions produce phase mixing (randomization) among ions leading to ion heating. After the phase mixing, the ions are stochastically heated by the mechanism discussed in this paper for the amplitude  $B_k^2/B_0^2 = 0.08$ , and the perpendicular temperature is much larger than the parallel temperature. The ions have large temperature anisotropy, which may excite ion cyclotron waves (Gary et al. 2003; Lu et al. 2006a, 2006b; Lu & Wang 2006). For the amplitude  $B_k^2/B_0^2 = 0.02$ , which is smaller than the threshold of the stochastic heating, there is no further heating.

### 3.2. The Alfvén Waves with Two Wave Modes

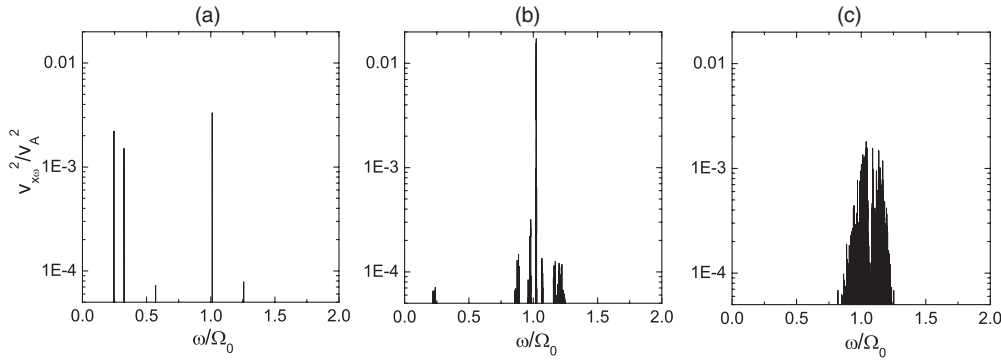
Here we consider the Alfvén waves with two wave modes, and their frequencies are  $0.25\Omega_p$  and  $0.33\Omega_p$ , respectively. They propagate along the same direction with  $\alpha = 45^\circ$ . The random phases of these two modes are  $0^\circ$  and  $30^\circ$ , respectively, and the ratio of their amplitudes is  $B_{k2}^2/B_{k1}^2 = 0.6295$ . With a spectrum consisting of waves with different frequencies, a Poincaré plot cannot be used to investigate the ion stochastic heating. However, similar to the Poincaré plot for the monochromatic Alfvén wave, we still can construct a plot of  $\lambda = v_z/v_A$ ,  $\psi_B = (\sum_k B_k \cos \psi_k)/\sum_k B_k$ , by taking points when  $v_y = 0$  and  $\dot{v}_y > 0$  in the wave frame. Figure 4 shows such plot for (a)  $\sum_k B_k^2/B_0^2 = 0.01$ , (b)  $\sum_k B_k^2/B_0^2 = 0.018$ , and (c)  $\sum_k B_k^2/B_0^2 = 0.04$ . Similar to Figure 1, which describes the results of the monochromatic wave case, with the increase of the wave amplitude, the  $z$  component of the ion velocity can be diffused to a large value. For example, the ion can be diffused from  $v_z = -v_A$  to about  $v_z = -0.95v_A$ ,  $-0.6v_A$ , and  $0.7v_A$  for the wave amplitude  $\sum_k B_k^2/B_0^2 = 0.01$ ,  $0.018$ , and  $0.04$ , respectively. The maximum value of  $v_z$  which the ion can be diffused to by the Alfvén waves increases abruptly around the amplitude  $\sum_k B_k^2/B_0^2 = 0.018$ . Therefore, we can suppose that the threshold for the ion stochastic heating is about  $\sum_k B_k^2/B_0^2 = 0.018$ .

Figure 5 shows the power spectrum of the  $x$  component of the ion velocity  $v_x(t)$ , which is obtained by FFT the time series of  $v_x(t)$  from  $\Omega_p t = 0$  to  $\Omega_p t = 26214.4$ , as in Figure 2. The parameters are the same as in Figure 4. When the wave amplitude is small ( $\sum_k B_k^2/B_0^2 = 0.01$ ), the ion motions have three main frequencies, and they are near  $0.25\Omega_p$ ,  $0.33\Omega_p$ , and  $1.0\Omega_p$ , respectively. The former two frequencies correspond to the frequencies of the Alfvén waves, and the last one corresponds to that of the ion gyromotion. The ion motions are quasi-periodic. When the wave amplitude is sufficiently large, the ion motions have a continuous frequency spectrum, and they are stochastic. Around  $\sum_k B_k^2/B_0^2 = 0.018$ , the spectrum becomes continuous, and the ion motions are stochastic. When  $\sum_k B_k^2/B_0^2 = 0.04$ , the continuous spectrum of the ion motions extends from  $0.75\Omega_p$  to  $1.3\Omega_p$ .

Figure 6 shows the time evolution of the parallel and perpendicular temperatures for the wave amplitude  $\sum_k B_k^2/B_0^2 = 0.01$  and  $\sum_k B_k^2/B_0^2 = 0.04$ . In the figure, A and B denote  $T_{\parallel}/T_{\parallel 0}$  and  $T_{\perp}/T_{\perp 0}$  for amplitude  $\sum_k B_k^2/B_0^2 = 0.01$ , while C and D denote  $T_{\parallel}/T_{\parallel 0}$  and  $T_{\perp}/T_{\perp 0}$  for amplitude  $\sum_k B_k^2/B_0^2 = 0.04$ . The initial



**Figure 4.** Plot of  $\lambda = v_z/v_A$ ,  $\psi_B = (\sum_k B_k \cos \psi_k)/\sum_k B_k$  for (a)  $\sum_k B_k^2/B_0^2 = 0.01$ , (b)  $\sum_k B_k^2/B_0^2 = 0.018$ , and (c)  $\sum_k B_k^2/B_0^2 = 0.04$ , by taking points when  $v_y = 0$  and  $\dot{v}_y > 0$  in the wave frame. The Alfvén waves have two wave modes, and their frequencies are  $0.25\Omega_0$  and  $0.33\Omega_0$ , respectively. They propagate along the same direction with  $\alpha = 45^\circ$ . The random phases of these two modes are  $0^\circ$  and  $30^\circ$ , respectively.



**Figure 5.** Power spectrum of the  $x$  component of the ion velocity  $v_x(t)$ , which is obtained by FFT the time series of  $v_x(t)$  from  $\Omega_p t = 0$  to  $\Omega_p t = 26214.4$ . The parameters are the same as in Figure 4.

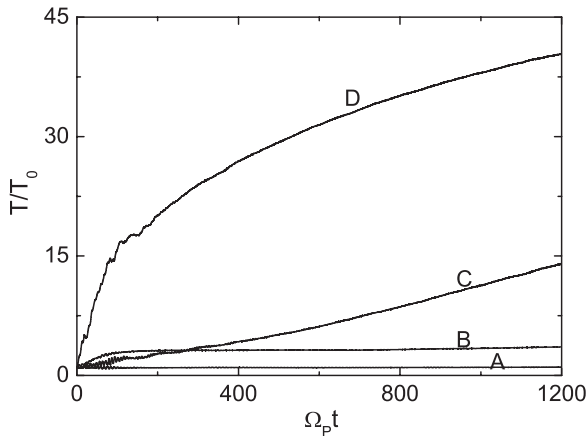


**Figure 6.** Time evolution of the parallel and perpendicular temperatures for the wave amplitude  $\sum_k B_k^2/B_0^2 = 0.01$  and  $\sum_k B_k^2/B_0^2 = 0.04$ . The Alfvén waves have two wave modes, and their frequencies are  $0.25\Omega_0$  and  $0.33\Omega_0$ , respectively. They propagate along the same direction with  $\alpha = 45^\circ$ . The random phases of these two modes are  $0^\circ$  and  $30^\circ$ , respectively. In the figure, A and B denote  $T_{\parallel}/T_{\parallel 0}$  and  $T_{\perp}/T_{\perp 0}$  for amplitude  $\sum_k B_k^2/B_0^2 = 0.01$ , while C and D denote  $T_{\parallel}/T_{\parallel 0}$  and  $T_{\perp}/T_{\perp 0}$  for amplitude  $\sum_k B_k^2/B_0^2 = 0.04$ .

and boundary conditions are the same as discussed in the above subsection. Similar to the case with the monochromatic Alfvén wave, we can find that ions can be rapidly heated by phase mixing before  $\Omega_p t \approx 100$ . Then the ions are stochastically heated by the mechanism for the amplitude  $\sum_k B_k^2/B_0^2 = 0.04$ , and they have temperature anisotropy with the perpendicular temperature much larger than the parallel temperature. However, for the amplitude  $\sum_k B_k^2/B_0^2 = 0.01$ , there is no further heating after  $\Omega_p t \approx 100$ .

We also consider the effects of the amplitude ratio  $B_{k2}^2/B_{k1}^2$  on ion motions by keeping  $\sum_k B_k^2/B_0^2$  as a constant. Figure 7 shows a plot of  $\lambda = v_z/v_A$ ,  $\psi_B = (\sum_k B_k \cos \psi_k)/\sum_k B_k$ , by taking points when  $v_y = 0$  and  $\dot{v}_y > 0$  in the wave frame for (a)  $B_{k2}^2/B_{k1}^2 = 0.1$ , (b)  $B_{k2}^2/B_{k1}^2 = 0.17$ , and (c)  $B_{k2}^2/B_{k1}^2 = 0.4$ , while  $\sum_k B_k^2/B_0^2$  is kept as 0.04. With the increase of the amplitude  $B_{k2}^2$ , the ion motions tend to be stochastic. Around  $B_{k2}^2/B_{k1}^2 = 0.17$ , the ion motions become stochastic, and the  $z$  component of the ion velocity can be diffused from  $v_z = -v_A$  to about  $v_z = 0.6v_A$ . When  $B_{k2}^2$  approaches to  $B_{k1}^2$ , the stochasticity of the ion motions increases. For  $B_{k2}^2/B_{k1}^2 = 0.4$ ,  $v_z$  can be diffused from  $v_z = -v_A$  to about  $v_z = 0.7v_A$ . This can also be demonstrated in Figure 8, which describes the power spectrum of the  $x$  component of the ion velocity  $v_x(t)$ , which is obtained by

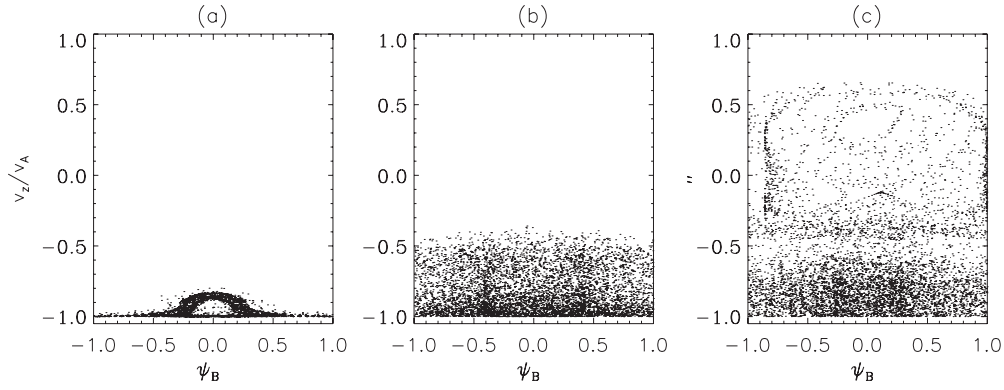
FFT the time series of  $v_x(t)$  from  $\Omega_p t = 0$  to  $\Omega_p t = 26214.4$ , as in Figure 2. The parameters are the same as in Figure 7. When the amplitude ratio is small ( $B_{k2}^2/B_{k1}^2 = 0.1$ ), the ion motions have several distinct frequencies. The main frequencies concentrate on about  $0.25\Omega_p$  and  $1.0\Omega_p$ , respectively, which correspond to the main frequency of the Alfvén waves and the frequency of the ion gyromotion. The ion motions are quasi-periodic. The ion motions begin to have a continuous frequency spectrum for about  $B_{k2}^2/B_{k1}^2 = 0.17$ , and become stochastic.

### 3.3. The Alfvén Waves with a Spectrum

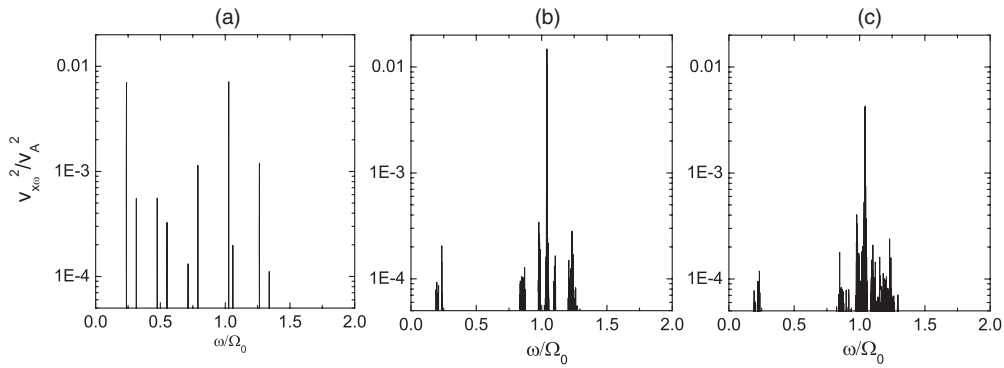
In order to investigate the effects of the number of wave modes on the ion motions, we keep  $\alpha = 45^\circ$  and  $\sum_k B_k^2/B_0^2 = 0.013$ . The frequencies of the waves extend from  $\omega_1 = 0.25\Omega_p$  to  $\omega_N = 0.33\Omega_p$ , and  $N$  is the number of wave modes used in our calculations. The frequencies of the wave modes can be calculated as follows:  $\omega_j = \omega_1 + (j-1)\Delta\omega$  ( $j = 1, 2, \dots, N$ ), where  $\Delta\omega = (\omega_N - \omega_1)/(N-1)$ . The amplitude of individual wave modes satisfies the relation  $(B_j/B_1)^2 = (\omega_j/\omega_1)^{-q}$ , and  $q$  is chosen as 1.667. This means that the power spectrum of the Alfvén waves has an index of  $-1.667$ , which is a generally accepted value for the power spectrum of magnetic fluctuations found in the solar wind (Villante 1980; Bavassano & Smith 1986). Figure 9 constructs a plot of  $\lambda = v_z/v_A$ ,  $\psi_B = (\sum_k B_k \cos \psi_k)/\sum_k B_k$ , by taking points when  $v_y = 0$  and  $\dot{v}_y > 0$  in the wave frame for (a)  $N = 1$ , (b)  $N = 2$ , (c)  $N = 5$ , and (d)  $N = 21$ . With the increase of wave modes, the ion motions become stochastic. From the figure, we can find that the ion motions for (c)  $N = 5$  and (d)  $N = 21$  are stochastic. This can also be verified in Figure 10, which shows the power spectrum of the  $x$  component of the ion velocity  $v_x(t)$  for (a)  $N = 1$ , (b)  $N = 2$ , (c)  $N = 5$ , and (d)  $N = 21$ . The power spectrum is obtained by FFT the time series of  $v_x(t)$  from  $\Omega_p t = 0$  to  $\Omega_p t = 26214.4$ , as in Figure 2. For (a)  $N = 1$  and (b)  $N = 2$ , the ion motions are quasi-periodic. It has several distinct frequencies, which correspond to that of the Alfvén wave modes and the ion gyromotion. For (c)  $N = 5$  and (d)  $N = 21$ , the ion motions which concentrate near Alfvén wave frequencies are very weak, while the motions near its gyromotion are very strong and its frequencies have a continuous spectrum. Therefore, its motions are stochastic. We also find that if we further increase the number of the wave modes, there is no obvious difference.

Figure 11 shows the time evolution of the parallel and perpendicular temperatures for different numbers of wave modes. In the figure, A and B denote  $T_{\parallel}/T_{\parallel 0}$  and  $T_{\perp}/T_{\perp 0}$  for the number of wave modes  $N = 2$ , while C and D denote  $T_{\parallel}/T_{\parallel 0}$  and  $T_{\perp}/T_{\perp 0}$  for the number of the wave modes  $N = 5$ . The other





**Figure 7.** Plot of  $\lambda = v_z/v_A$ ,  $\psi_B = (\sum_k B_k \cos \psi_k) / \sum_k B_k$ , by taking points when  $v_y = 0$  and  $\dot{v}_y > 0$  in the wave frame for (a)  $B_{k2}^2/B_{k1}^2 = 0.1$  (b)  $B_{k2}^2/B_{k1}^2 = 0.17$ , and (c)  $B_{k2}^2/B_{k1}^2 = 0.4$ , while  $\sum_k B_k^2/B_0^2$  is kept as 0.04. The Alfvén waves have two wave modes, and their frequencies are  $0.25\Omega_0$  and  $0.33\Omega_0$ , respectively. They propagate along the same direction with  $\alpha = 45^\circ$ . The random phases of these two modes are  $0^\circ$  and  $30^\circ$ , respectively.



**Figure 8.** Power spectrum of the  $x$  component of the ion velocity  $v_x(t)$ , which is obtained by FFT the time series of  $v_x(t)$  from  $\Omega_p t = 0$  to  $\Omega_p t = 26214.4$ . The parameters are the same as in Figure 7.

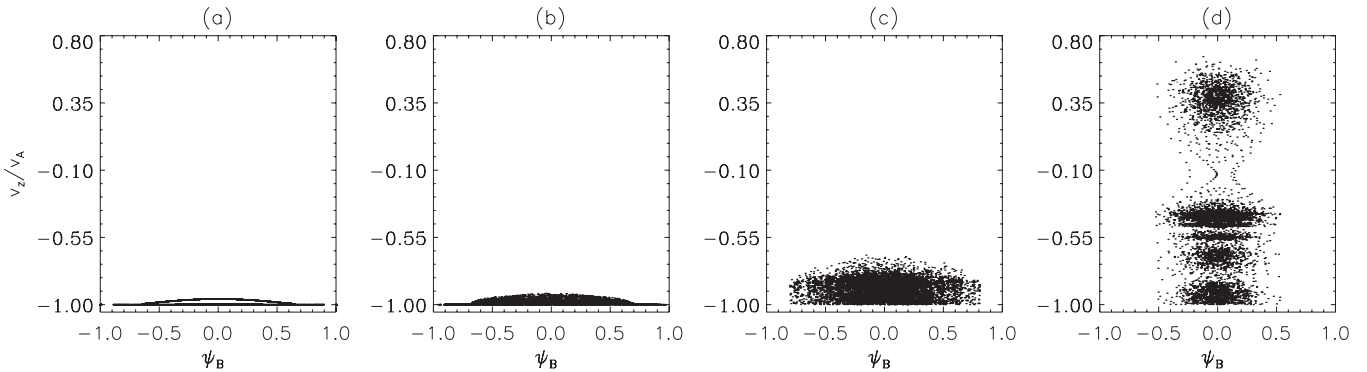


**Figure 9.** Plot of  $\lambda = v_z/v_A$ ,  $\psi_B = (\sum_k B_k \cos \psi_k) / \sum_k B_k$ , by taking points when  $v_y = 0$  and  $\dot{v}_y > 0$  in the wave frame for (a)  $N = 1$ , (b)  $N = 2$ , (c)  $N = 5$ , and (d)  $N = 21$ . We keep  $\alpha = 45^\circ$ , and  $\sum_k B_k^2/B_0^2 = 0.013$ . The frequencies of the waves extend from  $\omega_1 = 0.25\Omega_0$  to  $\omega_N = 0.33\Omega_0$ .

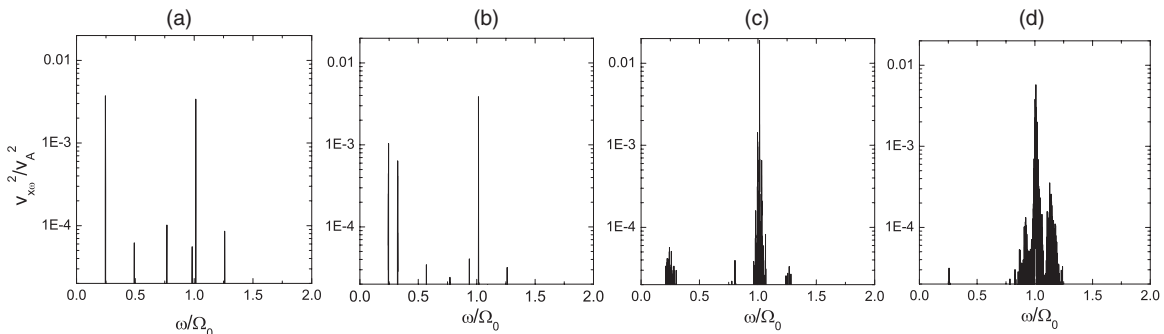


**Figure 10.** Power spectrum of the  $x$  component of the ion velocity  $v_x(t)$  for (a)  $N = 1$ , (b)  $N = 2$ , (c)  $N = 5$ , and (d)  $N = 21$ . The power spectrum is obtained by FFT the time series of  $v_x(t)$  from  $\Omega_p t = 0$  to  $\Omega_p t = 26214.4$ . The parameters are the same as in Figure 9.

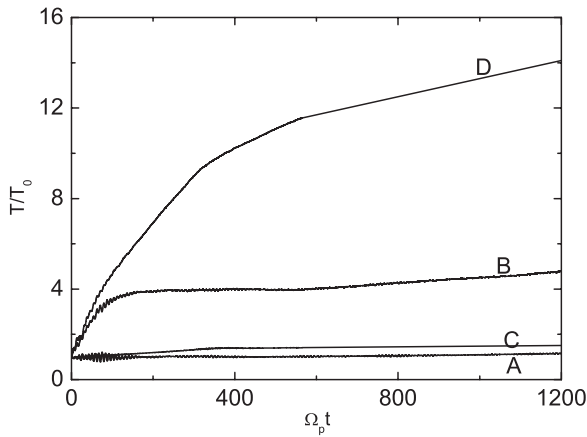


**Figure 11.** Time evolution of the parallel and perpendicular temperatures for different numbers of wave modes. In the figure, A and B denote  $T_{\parallel}/T_{\parallel 0}$  and  $T_{\perp}/T_{\perp 0}$  for the number of wave modes  $N = 2$ , while C and D denote  $T_{\parallel}/T_{\parallel 0}$  and  $T_{\perp}/T_{\perp 0}$  for the number of the wave modes  $N = 5$ . The other parameters are the same as in Figure 9.

parameters are the same as in Figure 9. The initial and boundary conditions are the same as discussed in the above subsections. Similar to the cases in the above subsections, we can find that ions can be rapidly heated by phase mixing before  $\Omega_p t \approx 100$ . Then, for  $N = 5$ , the ions are stochastically heated with large temperature anisotropy. However, for  $N = 2$ , no further heating can be found after  $\Omega_p t \approx 100$ .

Figure 12 shows that the threshold of ion stochastic motions for the different number of wave modes and frequencies, (a) is for  $\alpha = 45^\circ$  and (b) for  $\alpha = 60^\circ$ . The range for the frequencies is kept as  $\omega_N - \omega_1 = 0.08\Omega_0$ . In general, with the increase of the number of wave modes, the threshold decreases, especially for the low-frequency waves. Therefore, if a spectrum of waves is considered, the threshold can be much lower than that of a monochromatic wave. When the number of wave modes is sufficiently large, there is no obvious difference. With the increase of the wave frequencies and the propagation angle  $\alpha$ , the threshold of ion stochastic motions decreases. In summary, if a spectrum of Alfvén waves is considered, the threshold of ion stochastic motions can be much lower than that of the monochromatic wave. For example, for  $\omega_1 = 0.05\Omega_0$ ,  $N = 21$ ,  $\alpha = 45^\circ$ , the threshold of amplitude can be as low as  $\sum_k B_k^2/B_0^2 = 0.052$ . We can also find that with the increase of the propagation angle  $\alpha$ , the ions can be stochastically heated with more efficiency. Figure 13 shows the time evolution of the parallel and perpendicular temperatures

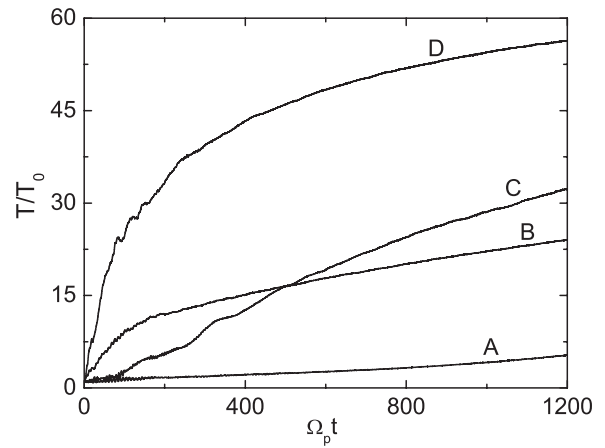


**Figure 13.** Time evolution of the parallel and perpendicular temperatures for different propagation angle  $\alpha$ , the amplitude of Alfvén waves is  $\sum_k B_k^2/B_0^2 = 0.028$  with the number of the waves modes  $N = 2$ , and the other parameters are the same as in Figure 9. In the figure, A and B denote  $T_{\parallel}/T_{\parallel 0}$  and  $T_{\perp}/T_{\perp 0}$  for the propagation angle  $\alpha = 45^\circ$ , while C and D denote  $T_{\parallel}/T_{\parallel 0}$  and  $T_{\perp}/T_{\perp 0}$  for the propagation angle  $\alpha = 60^\circ$ .

for different propagation angle  $\alpha$ , the amplitude of Alfvén waves is  $\sum_k B_k^2/B_0^2 = 0.028$  with the number of the waves modes  $N = 2$ , and the other parameters are the same as in Figure 9. In the figure, A and B denote  $T_{\parallel}/T_{\parallel 0}$  and  $T_{\perp}/T_{\perp 0}$  for the propagation angle  $\alpha = 45^\circ$ , while C and D denote  $T_{\parallel}/T_{\parallel 0}$  and  $T_{\perp}/T_{\perp 0}$  for the propagation angle  $\alpha = 60^\circ$ . Obviously, the heating of the ions is more efficient for the propagation angle  $\alpha = 60^\circ$ .

#### 4. SUMMARY AND DISCUSSION

Extended from the paper of Chen et al. (2001), we investigate the ion stochastic heating by a spectrum of low-frequency Alfvén waves, which are left-hand polarized and propagate obliquely to the background magnetic field. The results show that when a spectrum of Alfvén waves is considered, the threshold of ion stochastic heating is much lower than that of the monochromatic wave. Even when the frequencies of Alfvén waves are several percent of the ion cyclotron frequency, ions may also be stochastically heated. When the amplitude of the waves is sufficiently large, the velocity of the ion stochastic motions has a continuous spectrum of frequencies near the ion cyclotron frequency due to the nonlinear coupling between the ion gyromotion and the Alfvén waves, which leads to ion stochastic motions.

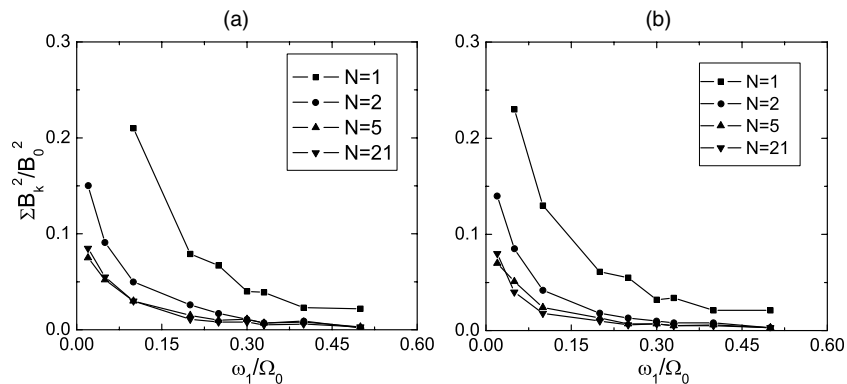


**Figure 12.** Threshold of ion stochastic motions for the different number of wave modes and frequencies, (a) is for  $\alpha = 45^\circ$  and (b) for  $\alpha = 60^\circ$ . The range for the frequencies is kept as  $\omega_N - \omega_1 = 0.08\Omega_0$ .

Low-frequency Alfvén waves are thought to be pervasive in the solar corona (Belcher et al. 1969; Tu & Marsch 2001). The energy of these low-frequency Alfvén waves can be transferred to that of higher frequencies by the perpendicular cascade in incompressible MHD turbulence (see, e.g., Cranmer & van Ballegoijen 2003 and references therein), or by three-wave interactions in compressible MHD turbulence with the existence of fast magnetosonic waves (Chandran 2005). The perpendicular cascade can lead to Alfvén waves to have wavevectors perpendicular to the background magnetic field. Then, the mechanisms of ion stochastic heating discussed in this paper may have relevance with solar corona heating.

The authors acknowledge useful discussions with Zehua Guo. Q.M.L. acknowledges support of the National Science Foundation of China (40725013, 40674093), and Chinese Academy of Science (KJCX2-YW-N28). L.C. acknowledges support of US DoE and NSF grants, and National Basic Research of China under Grant No. 2008CB717806.

#### REFERENCES

- Abe, H., et al. 1984, *Phys. Rev. Lett.*, **53**, 1153  
 Bavassano, B., & Smith, E. J. 1986, *J. Geophys. Res.*, **91**, 1706  
 Belcher, J. W., Davis, L. J., & Smith, E. J. 1969, *J. Geophys. Res.*, **74**, 2302  
 Birdsall, C. K., & Langdon, A. B. 2005, *Plasma Physics via Computer Simulations* (Bristol: Institute of Physics Publishing)  
 Chandran, B. D. G. 2005, *Phys. Rev. Lett.*, **95**, 265004  
 Chen, L., Lin, Z. H., & White, R. B. 2001, *Phys. Plasmas*, **8**, 4713  
 Cranmer, S. R., Field, G. B., & Kohl, J. L. 1999, *ApJ*, **518**, 937  
 Cranmer, S. R., & van Ballegoijen, A. A. 2003, *ApJ*, **594**, 573  
 Fredrickson, E. D., et al. 2002, *Phys. Plasmas*, **9**, 2069  
 Gary, S. P., et al. 2003, *J. Geophys. Res.*, **108**, 1068  
 Gates, D. A., Gorelenkov, N. N., & White, R. B. 2001, *Phys. Rev. Lett.*, **87**, 205003  
 Guo, Z. H., Crabtree, C., & Chen, L. 2008, *Phys. Plasmas*, **15**, 032311  
 Hollweg, J. V. 1978, *Rev. Geophys. Space Phys.*, **16**, 689  
 Isenberg, P. A., & Hollweg, J. V. 1983, *J. Geophys. Res.*, **88**, 3923  
 Karney, C. F. F. 1979, *Phys. Fluids*, **22**, 2188  
 Li, X., Lu, Q. M., & Li, B. 2007, *Astrophys. Lett.*, **661**, L105  
 Li, X., et al. 1999, *J. Geophys. Res.*, **104**, 2521  
 Lieberman, M. A., & Lichtenberg, A. J. 1973, *Plasma Phys.*, **15**, 125  
 Lieberman, M. A., & Lichtenberg, A. J. 1983, *Regular and Chaotic Dynamics* (New York: Springer)  
 Lu, Q. M., Guo, F., & Wang, S. 2006a, *J. Geophys. Res.*, **111**, A04207  
 Lu, Q. M., & Li, X. 2007, *Phys. Plasmas*, **14**, 042303  
 Lu, Q. M., & Wang, S. 2006, *J. Geophys. Res.*, **111**, A05204  
 Lu, Q. M., Xia, L. D., & Wang, S. 2006b, *J. Geophys. Res.*, **111**, A09101  
 Nekrasov, A. K. 1970, *Nucl. Fusion*, **10**, 387  
 Tu, C. Y., & Marsch, E. 2001, *J. Geophys. Res.*, **106**, 8233  
 Villante, U. 1980, *J. Geophys. Res.*, **85**, 6869  
 White, R. B., Chen, L., & Lin, Z. H. 2002, *Phys. Plasmas*, **9**, 1890  
 Zhang, Y., et al. 2008, *Phys. Plasmas*, **15**, 012103